

In situ synthesis of NiS/Ni₃S₂ nanorod composite array on Ni foil as a FTO-free counter electrode for dye-sensitized solar cells

Yongping Liao, Kai Pan*, Qingjiang Pan, Guofeng Wang, Wei Zhou, Honggang Fu*

Key Laboratory of Functional Inorganic Material Chemistry, Ministry of Education,
Heilongjiang University, Harbin 150080, People's Republic of China

Tel.: +86 451 8660 9141; fax: +86 451 8667 3647;

E-mail: kaipan@hlju.edu.cn, fuhg@vip.sina.com

1. Chemicals

The sulfur powder (99%, Tianli, Tianjin), nickel foil (99%, Maikun, Shanghai), cetyltrimethyl ammonium bromide (CTAB, 99%, Huishi, Shanghai), aqueous hydrazine (99%, Xilong, Guangdong), the commercial TiO₂ powder (P25, Degussa, Germany) were purchased from standard source. Fluorine doped SnO₂ (FTO) glass (20 Ω/square, Nippon sheet glass, Japan) was used as electrode substrate. The used Ru complex dye was cis-bis(isothiocyanato) bis (2,2' -bipyridyl-4,4' -dicarboxylato) ruthenium (II) bistetrabutylammonium (N719, Solaronix SA, Switzerland). The redox shuttle electrolyte was a blend of 0.1 M LiI (anhydrous, 99%, Acros), 0.05 M I₂ (anhydrous, 99.8%), 0.5 M tertbutylpyridine (99%, Aldrich) and 0.6 M 0.6 M 1-propyl-2, 3-dimethylimidazolium iodide (99%) in acetonitrile (99%, Fluka). All the chemicals were used as received without further purification.

2. Synthesis of NiS/Ni₃S₂ nanorod composite array CEs

The NiS/Ni₃S₂ nanorod composite array CEs were prepared similar to the reported procedure^{S1}, just adjusting the ratio of Ni foil and sulfur powder. In detail, a piece of Ni foil (thickness: 0.15mm; 1.5 cm×2.5 cm), 2 mmol of sulfur powder and 1.1 mmol of CTAB were introduced into a 40 mL Teflon-lined autoclave, then 28 mL of deionized (DI) water and 2 mL aqueous hydrazine were added, the autoclave was heated at 180 °C for 12 h and then cooled to room temperature. The nickel foil was taken out of solution, washed with ethanol, and finally air-dried for characterization. As a comparison, the hierarchical Ni₃S₂ CEs was synthesized with the absence of

CTAB and aqueous hydrazine. The NiS CEs on Ni foil were also fabricated via the reported method^{S3}. A mirror-like Pt cathode was fabricated by pyrolysis of H₂PtCl₆ isopropanol solution at 385 °C for 30 min^{S2}.

3. Assembly of DSSCs

The dye-sensitized TiO₂ photoanodes were prepared according to previous work^{S4}. The photoanodes and CEs were adhered together with epoxy resin, then, the redox shuttle electrolyte was injected into the space between the photoanodes and CEs.

4. Characterization

The composition of the composite nanomaterials was studied by X-ray diffraction (XRD), which was recorded using a Rigaku D/max-III B diffractometer with Cu K α (λ = 1.5406 Å). X-ray photoelectron spectroscopy (XPS) analysis was performed on a VG ESCALAB MK II with an Mg K α (1253.6 eV) achromatic X-ray source. Scanning electron microscopy (SEM, Hitachi, S-4800). Transmission electron microscopy (TEM) experiment was performed on a JEM-3010 electron microscope (JEOL, Japan) with an acceleration voltage of 200 kV. Carbon-coated copper grids were used as the sample holders. The scanning Kelvin probe (SKP) measurements (SKP5050 system, Scotland) have been performed at normal conditions of laboratory (in ambient atmosphere). A gold electrode was used as the reference electrode and the air gap between probe and sample was kept at 70 μm.

Photovoltaic measurements were carried out with a solar simulator (Oriel, USA) equipped with an AM 1.5G filter (Oriel, USA). The power of the simulated light was calibrated to 100 mW cm⁻² by using a solar simulator radiometer (Oriel, USA). Photocurrent–photovoltage (J-V) curves were obtained with a BAS100B electrochemical analyzer (Bioanalytical Systems Inc., USA) by applying an external photo-mask of 0.12 cm². The electrochemical impedance spectroscopy (EIS) experiments were conducted with a symmetric cell consisting of two identical CEs by using a computer-controlled potentiostat (Zahner Elektrik, Germany), and carried out by applying sinusoidal perturbations of 10 mV under bias of 0V in the dark, and the frequency ranges from 10 mHz to 1 MHz. The obtained spectra were fitted with ZsimpWin software in terms of appropriate equivalent circuits. The Tafel polarization

measurements were carried out with BAS100B electrochemical analyzer in a symmetric cell with a scan rate of 50 mV s^{-1} . The cyclic voltammetry (CV) curves were carried out in a three-electrode system in a nitrogen-purged acetonitrile solution, which contains 0.1 M LiClO_4 , 10 mM LiI and 1 mM I_2 , at a scan rate of 25 mV s^{-1} with BAS100B electrochemical analyzer, thereinto, Pt worked as an auxiliary electrode, versus the Ag/Ag^+ reference electrode.

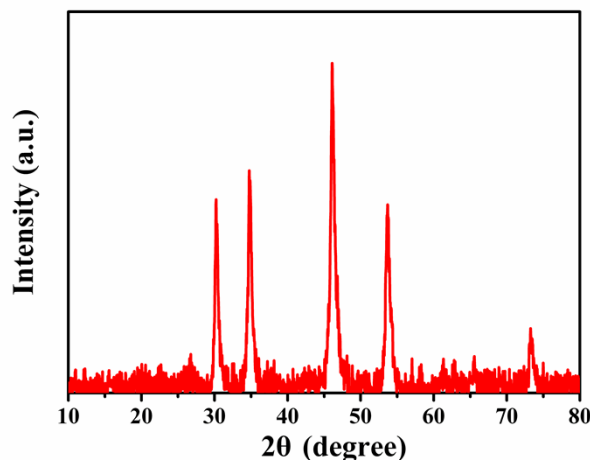


Fig. S1 XRD pattern of the NiS

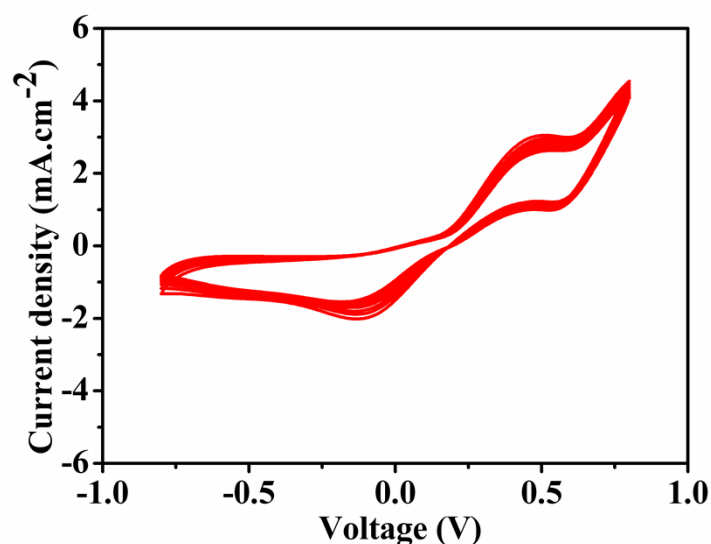


Fig. S2 Consecutive 20 cyclic voltammograms for the $\text{NiS}/\text{Ni}_3\text{S}_2$ nanocomposite cathode at a scan rate of 25 mV s^{-1} .

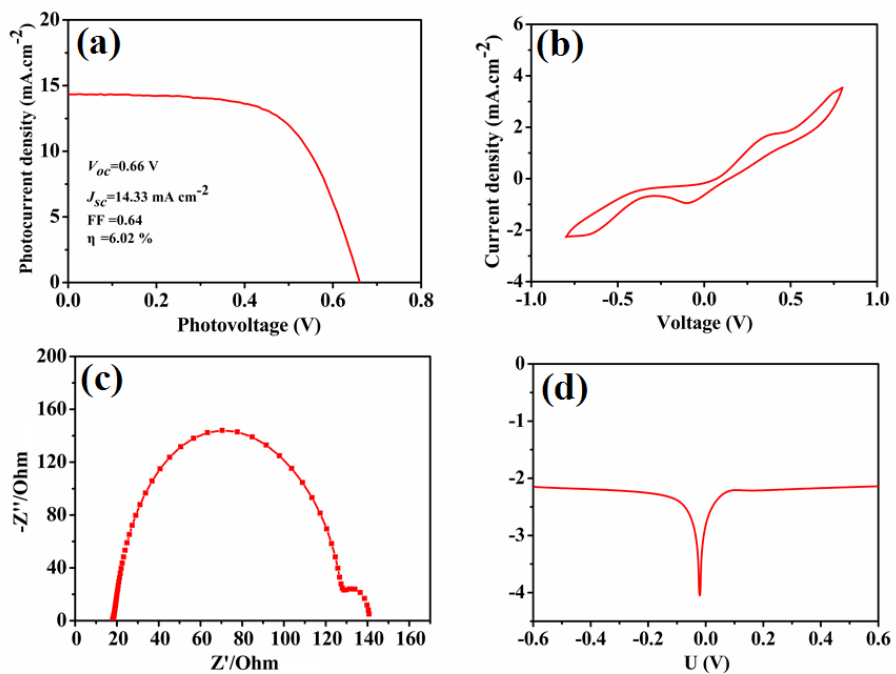


Fig. S3 (a) J - V characteristics of DSSCs with NiS CEs, (b) Cyclic voltammogram for the NiS CEs at a scan rate of 25 mV s⁻¹, (c) Nyquist plot of NiS symmetric cell, (d) Tafel-polarization curve of the NiS symmetric cell.

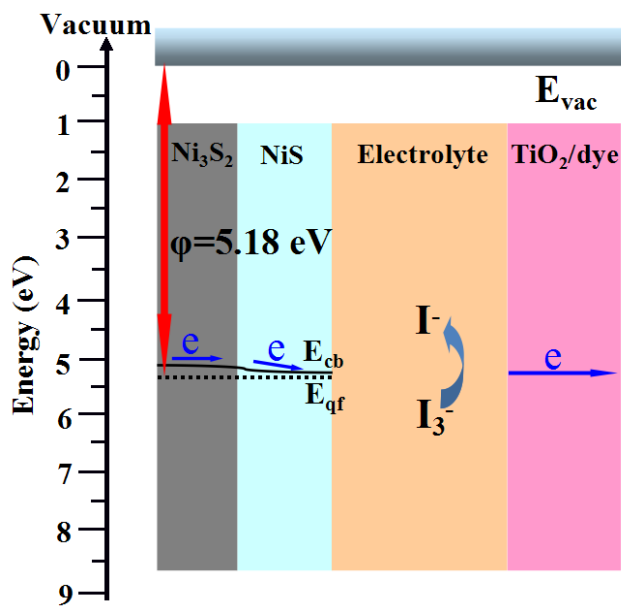


Fig. S4 The energy level of NiS/Ni₃S₂ electrode.

Table S1. The reported efficiency of DSSCs based on nickel sulfide counter electrodes.

CE materials	Method of preparing CE	η_{CE} (%)	η_{Pt} (%)	η_{CE} / η_{Pt}	Ref.
NiS nanoparticles	Drop casted on FTO	6.8	5.8	1.17	S3
NiS nanoparticles	Electrochemical deposition on FTO	6.83	7.00	0.98	S5
Ni ₃ S ₂ nanoparticles	Drop casting the precursor on FTO then annealed	7.01	7.32	0.96	S6
NiS nanowall	In-situ grown on Ni foam by hydrothermal method	8.55	7.99	1.07	S7
NiS nanorods	One-pot hydrothermal method on FTO	7.41	7.55	0.98	S8
NiS nanoparticles	In-situ grown on FTO by hydrothermal method	6.81	6.85	0.99	S9
{0001} faceted single crystal NiS nanosheet	In-situ grown on FTO by hydrothermal method	9.62	7.36	1.17	S10
NiS / Ni ₃ S ₂ hybrid nanorods	In-situ grown on Ni foil by hydrothermal method	7.20	7.56	0.95	Our work

References

S1. L. Z. Zhang, J. C. Yu, M. S. Mo, L. Wu, Q. Li and K. W. Kwong, *J. Am. Chem. Soc.*, 2004, **126**, 8116–8117.

S2. A. Hagfeldt and M. Grätzel, *Acc. Chem. Res.*, 2000, **33**, 269–277.

S3. W. S. Chi, J. W. Han, S. Yang, D. Y. Roh, H. Lee and J. H. Kim, *Chem. Commun* 2012, **48**, 9501–9503.

S4. M. K. Nazeerudin, A. Kay, I. Rodicioet, R. H. Baker, E. Müller, P. Liska, N. Vlachopoulos and M. Grätzel, *J. Am. Chem. Soc.*, 1993, **115**, 6382–6390.

S5. H. C. Sun, D. Qin, S. Q. Huang, X. Z. Guo, D. M. Li, Y. H. Luo and Q. B. Meng, *Energy Environ. Sci.*, 2011, **4**, 2630–2637.

S6. H. K. Mulmudi, S. K. Batabyal, M. Rao, N. Mathews, Y. M. Lam and S. G. Mhaisalkar, *Phys. Chem. Chem. Phys.*, 2011, **13**, 19307–19309.

S7. W. J. Ke, G. J. Fang, H. Tao, P. L. Qin, J. Wang, H. W. Lei, Q. Liu and X. Z. Zhao, *ACS Appl. Mater. Interfaces*, 2014, **6**, 5525–5530.

S8. W. Zhao, T. Q. Lin, S. R. Sun, H. Bi, P. Chen, D. Y. Wan and F. Q. Huang, *J. Mater. Chem. A*, 2013, **1**, 194–198.

S9. J. Yang, C. X. Bao, K. Zhu, T. Yu, F. M. Li, J. G. Liu, Z. S. Li and Z. G. Zou, *Chem. Commun.*, 2014, **50**, 4824–4826.

S10. Y. B. Li, H. F. Wang, H. M. Zhang, P. R. Liu, Y. Wang, W. Q. Fang, H. G. Yang, Y. Li and H. J. Zhao, *Chem. Commun.*, 2014, **50**, 5569–5571.